SYNCHROINFO JOURNAL

www.media-publisher.eu/synchroinfo-journal

OUTPHASING POWER AMPLIFIER EFFICIENCY

Quoc Fung Ngo [1], Oleg V. Varlamov [1,2,*]

[1] Moscow Technical University of Communications and Informatics, Moscow, Russia;
[2] Institute of Radio and Information Systems (IRIS), Vienna, Austria; vov@mtuci.ru
* Correspondence: vov@mtuci.ru

ABSTRACT

This article examines the operating characteristics of channel generators in outphasing high-efficiency radio-frequency power amplifiers. It demonstrates the advantage of using Voltage Mode Class D (VMCD) switching generators with filter loads (FL) on field-effect (FET) transistors – MOSFETs, VDMOS, LDMOS, and GaN HEMTs. Based on equivalent circuits and currents and voltages diagrams, basic expressions are derived for calculating output power, power loss, efficiency, and maximum currents when operating with matched and mismatched (complex) loads. The presence of inverse currents is demonstrated, and their maximum values, achievable with a 45-degree phase shift, are determined, which are necessary for selecting the component base.

DOI: 10.36724/2664-066X-2026-12-4-19-31

Received: 15.04.2026
Accepted: 27.06.2026

KEYWORDS: *outphasing power amplifier; energy efficiency; switching generator; Voltage Mode Class D; filter loads; field-effect transistor; equivalent circuits; mismatched loads; inverse currents.*

Citation: Q.F. Ngo, O.V. Varlamov, "Outphasing power amplifier efficiency," *Synchroinfo Journal* **2026**, vol. 12, no. 4, pp.19-31.

Licensee IRIS, Vienna, Austria.

This article is an open access article distributed under the terms and conditions of the Creative Commons Attribution (CC BY) license (https://creativecommons.org/licenses/by/4.0/).

Copyright: © 2026 by the authors.

1 Introduction

High-efficiency radio-frequency power amplifiers built using the outphasing method (OPA) [1, 2] with channel power direct summation [3, 4] have good prospects for use in modern telecommunications systems. They exhibit sufficient linearity [5-7] to amplify signals with high crest factors, such as OFDM, for digital television [8] and radio broadcasting [9, 10], satellite applications [11-13], and others. Unlike other "synthetic" high-efficiency amplification methods (envelope elimination and restoration - EER, envelope tracking - ET), OPA does not contain a powerful modulation path [14, 15], which reduces efficiency and limits the amplified frequency band and antenna matching requirements [16, 17]. Therefore, the OPA is a good base element for the combined use of "synthetic" high-efficiency amplification methods [18-20]. However, a detailed examination of the OPA energy characteristics associated with power losses of various origins has not yet been conducted.

Based on the analysis of methods for two out-of-phase generators powers combining, conducted in [21] an important conclusion was reached: when generators in the switching (overvoltage) mode series summing, this mode is maintained with increasing phase shift between the driving signals up to 180^0, ensuring high generator efficiency. Therefore, it is proposed to design the final stages of outphasing transmitters using a series direct summation method. At the same time, as shown in [22], the change in the load delivered to the generators is very significant, caused by both the mutual phasing of the generators and the mismatch of the OPA's final load. This raises the problem of selecting, among known oscillator circuits, those switching generator variants that are least sensitive to load mismatch. After this, it is necessary to conduct a detailed analysis of the operating mode of the selected generator when used in the OPA's output stage, which will allow us to evaluate the power characteristics of the transmitter as a whole and develop recommendations for the channel amplifiers final stages design. This article is devoted to solving this problem.

2 Selecting Switching Oscillator for OPA Output Stage

Voltage Mode Class D (VMCD) oscillators with resistive (RL) and filter loads (FL) [23, 24] possess the required properties – operating as a voltage generator and maintaining their properties even with significant phase misalignment (up to 180 degrees) of the summed signals. Of these two types of switching oscillators, the VMCD with filter loads circuit is immediately preferable to the resistive load option, since the latter suffers from high harmonic power losses in the ballast resistance of the diplexer (filter plug), connected between the oscillator and the load to provide resistive loading of the oscillator for the first and higher harmonics [23].

At the same time, the construction of OPA output stages using VMCD FL switching generators is advisable only when the latter are built on field-effect (FET) transistors - MOSFET, VDMOS, LDMOS, GaN HEMT. This is due to two reasons. Firstly, as will be shown in the following sections, during outphasing (when operating on a resistive or complex load), the current pulses in the transistors become asymmetrical and bipolar, i.e. there are time intervals during which negative (inverse) current flows. Bipolar transistors ensure its flow significantly worse than FETs, and even the inclusion of special diodes [23] in parallel with the transistors output electrodes does not completely eliminate the consequences of this drawback. Secondly, in bipolar transistors, due to the relatively long carrier absorption time in the base-collector junction, when the transistor leaves the saturation state, overlap (expansion of the collector current pulses) occurs, which, in turn, leads to the appearance of shoot-through currents during time intervals when both switches are closed [22]. This phenomenon becomes especially noticeable when generators are operating on highly variable loads, which occurs during outphasing.

VMCD FL generators based on field-effect transistors, as follows from the fundamentals of the theory of their operation, should be free from the listed disadvantages. Thus, when field-effect transistors operate in the switching mode, there is no accumulation of charges and, therefore, the main reason for the occurrence of through currents is eliminated (strictly speaking, through currents in FET transistors can sometimes still occur, but for a completely different reason). In addition, field-effect transistors are switches with double-sided conductivity and allow the passage of inverse currents, which virtually eliminates the risk of surge currents and voltages and eliminates the need to bypass the output electrodes of transistors with additional diodes. Thus, VMCD FL generators based on field-effect MOSFET or GaN [25] transistors must maintain operability and high energy

characteristics with large changes in equivalent loads when operating in the OPA final stage.

Next, the operating mode of the VMCD FL generator is examined in detail when used in the OPA final stage, the features of this mode in the case of a large load mismatch are considered, and its energy characteristics are assessed.

3 Operation of the OPA Final Stage with a Matched Load

Let's consider the operation of push-pull switching oscillators VMCD FL (Fig. 1). When the switch is closed, a half-wave of the harmonic load current flows through it. It should be noted that the voltages at the transistor output electrodes differ from the voltages at the switches by the amount of the voltage drop across the resistor r_{sat}. When the switch is closed, the voltage drops across the switch itself is zero, and the voltage across the transistor is $U_{sat}(t) = r_{sat} * i_L(t)$. When the switch is open, almost the entire supply voltage $U(t) = E - U_{sat}(t)$ drops across the switch, and the current through it is zero. Fig. 2a) shows the current and voltage waveforms at the switches of the one OPA generator when operating with a resistive load R_L.

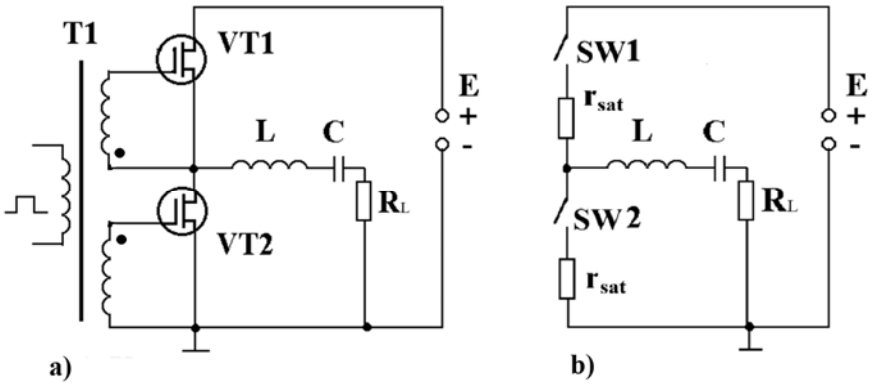


Figure 1. a) push-pull switching VMCD FL generator circuit;
b) simpli ed equivalent circuit

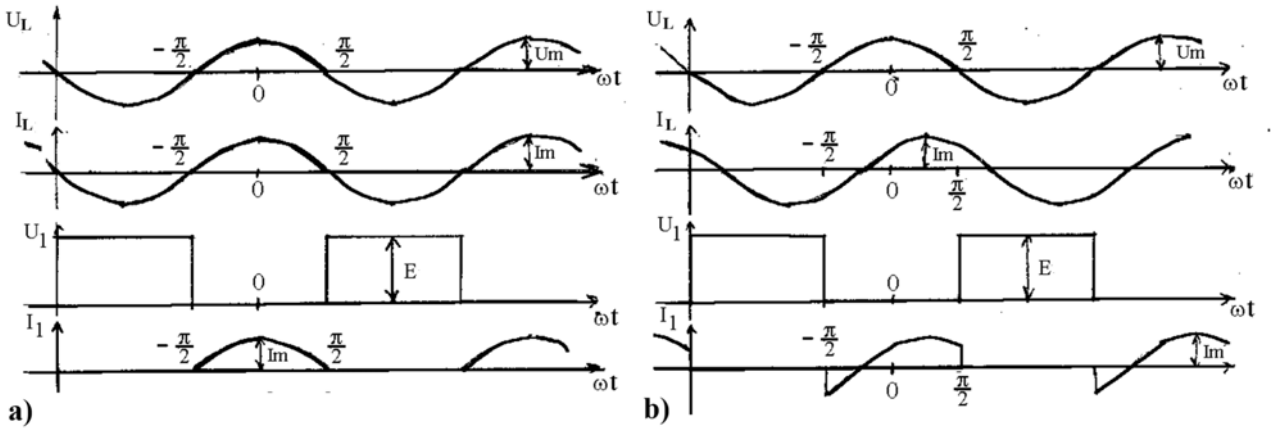


Figure 2. Current and voltage diagrams for one VMCD FL generator operating on resistive (a) and complex (b) loads

In the OPA final stage, two switching VMCD FL generators operate on a common load, which is reflected in the equivalent circuit shown in Figure 3. Here, each generator is represented by two switches (in one arm, switches 1.1 and 1.2, in the other, respectively, 2.1 and 2.2), with the saturation resistance of the transistors r_{sat} connected in series with each of them. Relative to the common filter load (L, C, R_L), the generators are connected in series. In the case of common-mode driving (when $2\varphi = 0$), the operating mode of both

generators is the same as that of a single generator (see the circuit in Fig. 1 and the diagrams in Fig. 2a). In this case, in the circuit in Figure 3, the diagonally located switches (switches 1.1, 2.2 and switches 1.2, 2.1) are switched in pairs in phase. In this case, the current and voltage diagrams for each of the switches of both generators coincide with the diagrams illustrating the operation of a single VMCD FL generator (Fig. 2a). The only difference lies in the magnitude of the reduced load resistances for each generator, which will be half the total load R_L (due to the fact that in the circuit under consideration, the generator powers are serially summed).

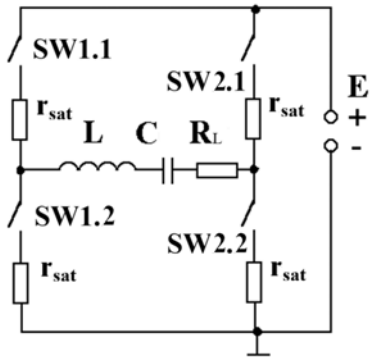


Figure 3. Output stage equivalent circuit of linear power amplifier using the outphasing method

With out-of-phase driving, the output voltage pulses and, accordingly, the first harmonics of the voltages on the switches $U_{SW}(t)$ of both generators (on switches 1.1 and 2.2 and, similarly, on switches 1.2 and 2.1) are shifted in phase relative to each other by the value 2φ, varying from 0 to 180 degrees according to the law determined by the OPA channel signal generator (Exciter) [26]. In this case, the pulse voltages and, accordingly, the first harmonics of the voltages on the switches relative to the output pulse voltage (voltages on the circuits L, C, RL) and its first harmonic are shifted by the value -φ for switches 1.1 and +φ for switches 2.2 (see Fig. 4).

In each switch, as at 2φ=0, the current $i_{sw}(t)$ flows for half the period. However, if at 2φ=0 this current is unipolar cosine pulses with a cutoff angle of 90^0 (as in the case of a single VMCD FL generator, see Fig. 2,a), then at 2φ>0 the switch current pulses $i_{sw}(t)$ are cosine segments of the same duration (φ), but with a phase shift φ. Thus, as can be seen from Figure 4, the pulses $i_{sw}(t)$ contain intervals where the current is negative (inverse). With increasing φ, the duration of these intervals increases and at $2\varphi \geq 180^0$ it approaches the duration of the intervals where the current is positive. In this case, the constant component in the current pulses decreases and at $2\varphi = 180^0$ it vanishes. At the same time, the output voltage pulses become infinitely short and the amplitude of the output signal is also zero. The corresponding current and voltage diagrams are shown in Figure 5. Thus, an analysis of Figure 4 and Figure 5 shows that with an increase in φ, the durations of the positive and negative output voltage pulses (voltages in the L, C, and R_L circuits) decrease and tend to zero at $2\varphi \rightarrow 180^0$. In this case, although the output voltage swing $U_{out}(t)$ remains unchanged and equal to 2E, the amplitude of the first harmonic voltage on the R_L load and the current in it tend to zero.

An interesting feature of the OPA output stage is that during intervals when the upper or lower pair of switches are closed, the load circuit is short-circuited by these switches, and the load current flows due to the energy stored in the output filter reactive elements. During these intervals, the power supply is disconnected from the load and delivers no power (no current flows through it). These features ensure OPA high efficiency with any phase shifts of the channel signals.

4 Operation of the OPA Final Stage with a Complex Load

As shown in the previous sections, with a complex load mismatch of a single VMCD FL generator (see Fig. 1), the load current lags or leads the phase of the voltages first harmonic on the switches. In this case, the current pulses in the switches become asymmetrical (see Fig. 2,b) and contain both positive and negative current sections (inverse current sections).

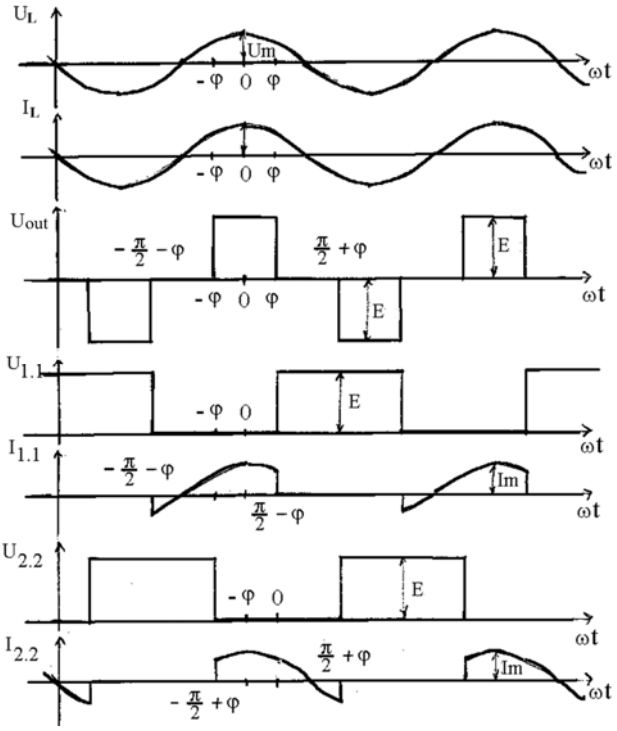


Figure 4. Current and voltage diagrams for VMCD FL generators operating on a resistive load during outphasing (φ>0)

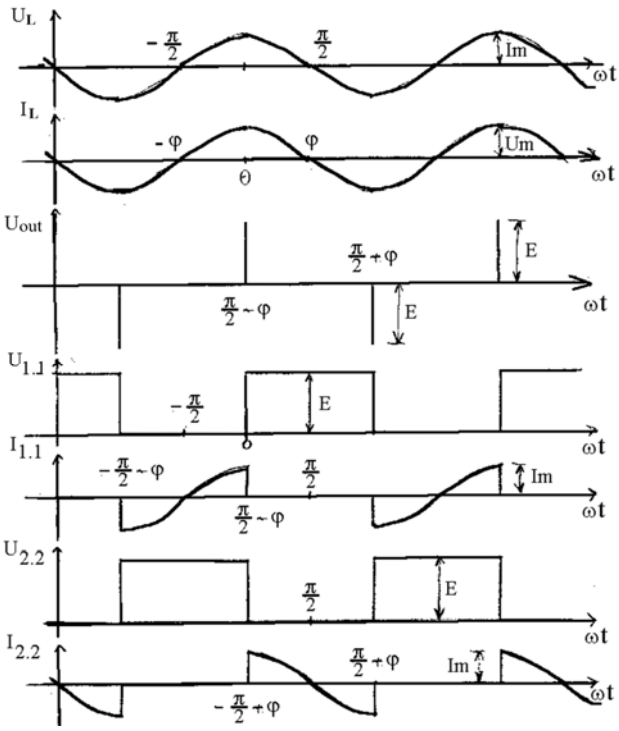


Figure 5. Current and voltage diagrams in the case of antiphase VMCD FL generators operation on a resistive load

In the OPA final stage (see the diagram in Fig. 3), with in-phase operation of two VMCD FL generators (2φ=0) and a common load mismatch, as with a single VMCD FL generator operating with a complex load, negative sections appear in the current pulses in the switches (inverse currents). When comparing the waveforms in Figure 2,b with those in Figure 4 shows that, while with a resistive load and outphasing, the phase shifts between the midpoints of the pulses and the first harmonics of the voltages on different switches and the maximum current in the load are equal in magnitude but opposite in sign. With a complex load and in-phase operation (2φ=0), the phase shifts are identical in both magnitude and sign in both generators. It follows that with outphasing and a complex load, the current pulses in the switches should have different shapes in different generators.

Thus, Figures 6 and 7 show the current and voltage waveforms on the switches under a complex load – inductive and capacitive, respectively. Depending on the sign of X_L, the current lags or leads the first harmonic of the total voltage, i.e., it has a certain phase shift χ relative to it and the current in the matched load. Note that the shape of the voltage pulses on the switches, as well as the shape of the total voltage from the two generators $U_{out}(\omega t)$, remains unchanged at $X_L \neq 0$, since we assume that the switching mode of the VMCD FL generators is maintained.

Figure 8 shows the pulse waveforms of currents and voltages on the switches for a very interesting special case, when the current in the load is in phase with the voltage on the switches of one of the VMCD FL generators, and the voltage on the switches of the other VMCD FL generator will be 90^0 out of phase (will be in quadrature) from the current in the load (i.e., for the case when $\varphi + \chi = \pi / 2$ or $-\varphi + \chi = 0$). In this case, the first generator works on a purely resistive load, and the second on a purely reactive one. When considering the waveforms for this case (see Fig. 8), it is easy to see that, indeed, for the current pulses of one of the switches, the sine (quadrature) component of the first harmonic vanishes (these pulses represent harmonic pulses with a cutoff angle of $\theta = 90^0$), while for the other, the cosine (in-phase) component vanishes.

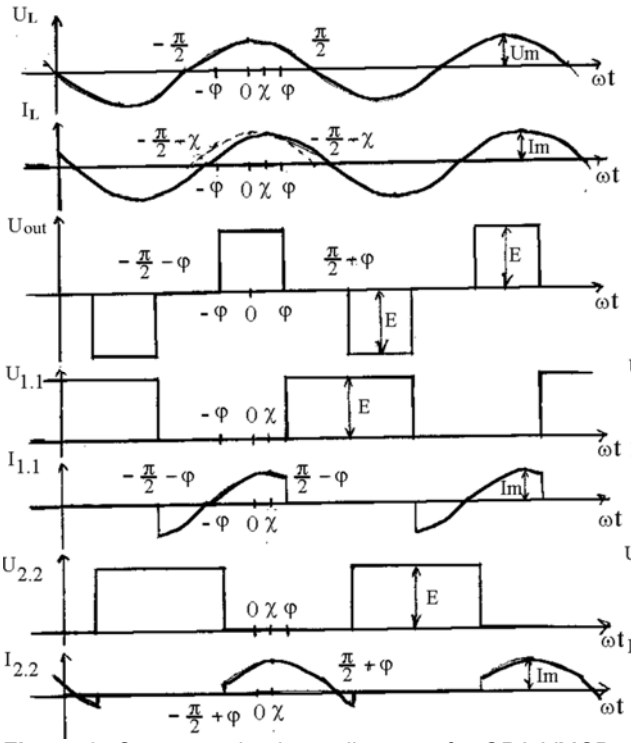


Figure 6. Current and voltage diagrams for OPA VMCD FL generators operating on a complex inductive load

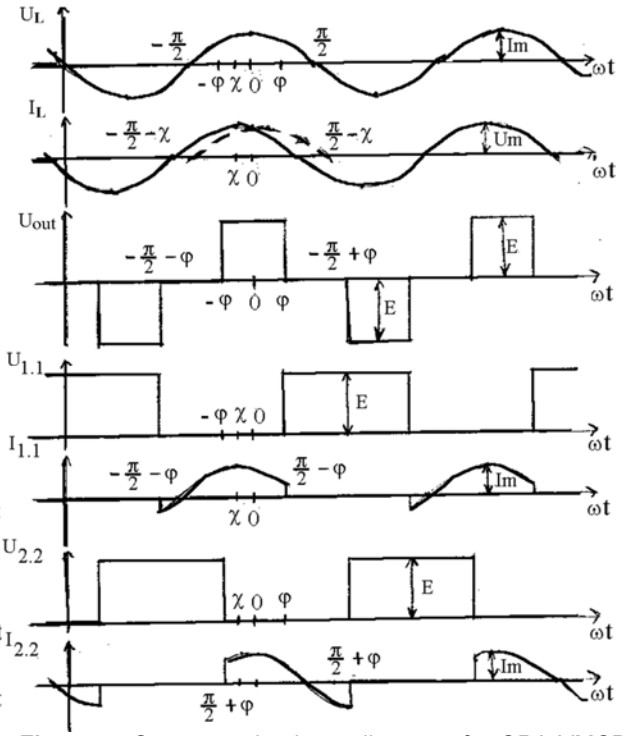


Figure 7. Current and voltage diagrams for OPA VMCD FL generators operating on a complex capacitive load

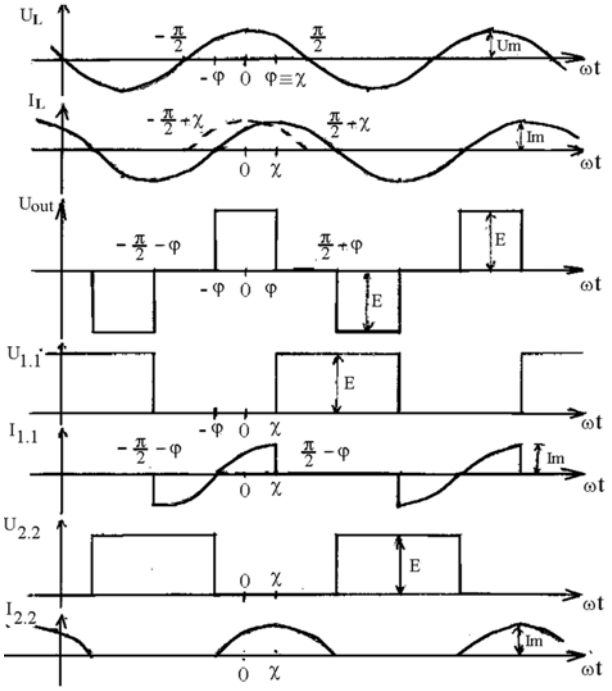


Figure 8. Current and voltage diagrams for OPA VMCD FL generators operating with a complex load – a special case

This indicates that one of the generators operates with a purely resistive load, while the other operates with a purely reactive load. In this case, the generator whose cosine (in-phase) component of the current pulses in the switches vanishes will not consume power from the power source, since in such pulses (see Fig. 8), the DC component is zero, meaning that the current consumed by the generator from the power source will also be zero. As φ increases, the DC component of the currents in the switches of this generator becomes negative. The current and power consumed by this generator also become negative, and it returns (recuperates) oscillatory power to the power supply. This, in turn, reduces the total power consumed and the power in the shared load of the two generators.

For such modes, as will be shown in Section 7, the efficiency of the OPA is virtually unchanged; the active device modes (currents and voltages at the drains of the output transistors) do not exceed their values at the point of maximum output power (common-mode mode) and are determined solely by the degree of mismatch in the shared load, as for a single VMCD FL generator [24].

5 Power Characteristics of the OPA Output Stage Operating with a Complex Load

To calculate OPA output stage power characteristics, we find expressions for the DC components of the currents in the switches, as well as the first harmonics of the voltages across them, according to the equivalent circuit in Figure 3, using the current and voltage diagrams in Figures 4...8. When deriving the relationships, we will limit ourselves to the analysis for switches 1.1 and 2.2 in the circuit in Figure 3, since the relationships for the other two switches will be similar. Expressions for the DC components of the currents in switches I_{0SW} of the generators are obtained by expanding the pulses of these currents in a Fourier series. Similarly, expressions for determining the amplitudes of the first harmonics of the voltages across switches U_{1SW} can be derived. In this case, we will assume that $Z_L \neq R_L$, which corresponds to the operation of two generators on a complex load (for the special case of a matched resistive load $Z_L = R_L$, it will be necessary to substitute $X_L = 0$ and $\chi = 0$ into the resulting relations).

The DC component of the current pulses in the switches is determined as follows:

$$I_{0SW} = 1/\pi \int_{-\pi/2\pm\varphi}^{\pi/2\pm\varphi} I_m \cos(\omega t + \chi) d\omega t\,, \tag{1}$$

Where I_m is the amplitude of the first harmonic of the load current (defined below).

After integrating (1), we obtain the desired expression for I_{0SW}.

$$I_{0SW} = \frac{I_m \cos(\chi \pm \varphi)}{\pi}. \tag{2}$$

The amplitude of the first harmonic contained in a rectangular pulse $u_{G1}(t)$ with a peak-to-peak amplitude E is determined as follows:

$$U^*_{G1i} = 1/\pi \int_{-\pi/2}^{\pi/2} u_{Gi}(t)\cos(\omega t)dt + 1/\pi \int_{-\pi/2}^{\pi/2} u_{Gi}(t)\sin(\omega t)dt\,, \tag{3}$$

$$U^*_{G1i} = 2\frac{E}{\pi}(\cos\varphi \pm J\sin\varphi)\,. \tag{4}$$

The "plus" sign in formulas (2) and (4) corresponds to switch SW1.1, and the "minus" sign corresponds to switch SW2.2.

As can be seen from (4), the amplitude of the first harmonic of the generator voltage is constant and independent of phase shifts, which becomes evident from an analysis of the time dependences of the voltages on the switches (see Fig. 4). At the same time, as can be seen from (2), the magnitudes of the DC components of the currents in the switches of different generators depend differently on the phase shift due to the complex load mismatch χ and, in general, are not equal in magnitude. This important circumstance will be discussed in more detail below in Section 7.

Expressions for voltage and current:

$$U_L = 4\frac{E}{\pi}\cos\varphi, \tag{5}$$

$$I_L^* = \left(4E\cos\varphi \bullet e^{-j\chi}\right) / \pi\sqrt{\left[\left(R_L + 2r_{sat}\right)^2 + X_L^2\right]}, \tag{6}$$

$$I_m = \left(4E\cos\varphi\right) / \pi\sqrt{\left[\left(R_L + 2r_{sat}\right)^2 + X_L^2\right]}. \tag{7}$$

Output power:

$$P_L = \left(8E^2\cos^2\varphi \bullet R_L\right) / \pi^2\left[\left(R_L + 2r_{sat}\right)^2 + X_L^2\right]. \tag{8}$$

Active power loss (per transistor):

$$P_{r_{sat}} = \left(8E^2\cos^2\varphi \bullet r_{sat}\right) / \pi^2\left[\left(R_L + 2r_{sat}\right)^2 + X_L^2\right]. \tag{9}$$

Voltage amplitude at the transistor saturation resistance:

$$U_{r_{sart}} = \left(4E\ \cos\ \varphi \bullet r_{sat}\right) / \pi\ \sqrt{\left[\left(R_L + 2r_{sat}\right)^2 + X_L^2\right]}. \tag{10}$$

The constant component of the currents in the switches, substituting (7) into (2):

$$I_{0SW} = \left(4E\cos\varphi \bullet \cos(\chi \pm \varphi)\right) / \pi^2\sqrt{\left[\left(R_L + 2r_{sat}\right)^2 + X_L^2\right]}. \tag{11}$$

Power consumed from the power supply:

$$\begin{aligned} P_0 &= 2E(I_{0SW1.1} + I_{0SW2.2}) = \\ &= \left(\left(4E^2\cos\varphi\right) / \pi^2\sqrt{\left[\left(R_L + 2r_{sat}\right)^2 + X_L^2\right]}\right) \times . \\ &\times \left(\cos(\chi + \varphi) + \cos(\chi - \varphi)\right) \end{aligned} \tag{12}$$

In case of resistive load:

$$P_0 = \left(8E^2\cos^2\varphi\right) / \pi^2\left(R_L + 2r_{sat}\right). \tag{13}$$

OPA output stage efficiency in the case of $Z_L = R_L$ and the commutation losses absence is determined from (3.8) and (3.13) as:

$$\eta = \frac{\mathrm{R}_L}{(\mathrm{R}_L + 2\cdot \mathrm{r}_{sat})} = \frac{1}{(1 + \frac{2\cdot \mathrm{r}_{sat}}{\mathrm{R}_L})} \tag{14}$$

Expression (14) differs from the expression that determines the efficiency of a single VMCD FL generator in [24] only by a factor of “2”. This is because the load current in the equivalent circuit in Figure 3 flows through two series-connected transistors (switches) with equal saturation resistances.

Thus, expressions (2), (4)...(14), describing currents, voltages and powers depending on the phase shift φ, make it possible to calculate the static modulation characteristics (SMC) of the OPA final stage, described by the equivalent circuit in Figure 3, and evaluate its energy performance.

6 Inverse Currents in the OPA Output Stage

When selecting transistors for VMCD FL switching generators, in addition to frequency limitations, it is important to consider that inverse currents flow through the transistors in OPA when the generators are out of phase. This section identifies the most dangerous point in the OPA output stage SMC, where the inverse current reaches its maximum value.

The ability of field-effect transistors to pass inverse currents significantly simplifies generators circuits with filter loads in the OPA output stages. At the same time, it is essential to be able to calculate the maximum value of these currents in order to select the appropriate transistors and ensure their safe operation.

As shown above, when two switching generators operate simultaneously in the OPA final stage, inversion sections appear in the switching current waveforms, with the maximum share of inversion current occurring when the generators operate in antiphase with a matched (resistive) load (see Fig. 5). At the same time, as the phase shift changes from 0 to 180 degrees, the amplitude of the currents (equal in magnitude to the load current amplitude) decreases according to the cosine law, according to (7), while the share of inversion current in the switches increases with increasing phase shift. Thus, the problem arises of finding the phase shift at which the maximum instantaneous value of inversion current is achieved, and then calculating this value.

Let us find the value of the phase angle φ for switch K2.2 in the equivalent circuit of Figure 3 for the case of the OPA operating with a matched load. Obviously, for the other three switches, the desired value will be the same. As can be seen from Figure 4, the inverse current reaches its maximum instantaneous value at the moment of time $\omega t = (\pi / 2) + \varphi$ and, accordingly, the current in the switch at this moment of time is equal to:

$$\mathrm{I}_{SW\,\frac{\pi}{2}+\varphi} = \mathrm{I}_{\mathrm{m}} \cdot \cos\left(\frac{\pi}{2}+\varphi\right). \quad (15)$$

Substituting the expression for the current amplitude (7) into (15) and assuming the load is matched, we obtain:

$$\mathrm{I}_{SW\,\frac{\pi}{2}+\varphi} = \frac{4 \cdot \mathrm{E} \cdot \cos\varphi \cdot \cos\left(\frac{\pi}{2}+\varphi\right)}{\pi^2 \cdot (\mathrm{R}_L + 2 \cdot \mathrm{r}_{sat})} = \frac{-2 \cdot \mathrm{E} \cdot \sin 2\varphi}{\pi^2 \cdot (\mathrm{R}_L + 2 \cdot \mathrm{r}_{sat})}. \quad (16)$$

Differentiating expression (16) with respect to φ and equating it to zero yields the expression

$$\frac{-4 \cdot \mathrm{E} \cdot \cos 2\varphi}{\pi^2 \cdot (\mathrm{R}_L + 2 \cdot \mathrm{r}_{sat})} = 0. \quad (17)$$

From the solution of which we find the value of the phase angle φ at which the inverse current reaches its maximum:

$$\varphi = \frac{\pi}{4}. \quad (18)$$

Taking the second derivative of expression (16) at this point and verifying that it is positive

$$\frac{8\cdot E\cdot\sin\frac{2\pi}{4}}{\pi^2\cdot(R_L+2\cdot r_{sat})}=\frac{8\cdot E}{\pi^2\cdot(R_L+2\cdot r_{sat})}>0, \quad (19)$$

we assume that we indeed have the current maximum.

Substituting (18) into (7), we obtain an expression for determining the maximum inverse current when the OPA operates with a matched load:

$$I_{INV_{max}}=\frac{2\cdot\sqrt{2}\cdot E}{\pi^2\cdot(R_L+2\cdot r_{sat})}. \quad (20)$$

Similarly, an expression can be derived for determining this value for the case of a complex load. Here it is necessary to take into account that the point of the minimum value of the current pulse will be shifted relative to this point in the case of a resistive load along the ωt axis by the value of the load phase χ and the current itself will have a phase shift of the same value (see diagrams in Fig. 6-8). Carrying out transformations similar to those described above, we obtain

$$\varphi=\frac{\pi}{4}-\chi. \quad (21)$$

Substituting (21) into expression (7), we can obtain an expression for I_{INVmax}. It should be noted that in the case of a complex load, this value turns out to be different for each of the two generators of the OPA final stage, depending on the sign of χ for each of them (see Fig. 6-8). As will be shown below (see Section 7), the emerging difference in the operating modes of channel generators is not dangerous if the transistors (MOSFET or GaN HEMT) are correctly selected for the maximum power mode for a given mismatch of the OPA total load.

7 Features of OPA Operation with Large Load Mismatches

Let's return to the operating mode of the OPA output stage, described by expression (11) and illustrated in Figure 8 when, due to a reactive load mismatch, the currents consumed by the generators are unequal. Using (11), normalized (relative to the point φ=0) dependences of these currents on the value of 2φ are plotted (Fig. 9) for a fixed value of $\chi=\pi/4$. These theoretical curves correspond to the special case considered above, which is illustrated by the diagrams in Figure 8. In this case, the voltage of one of the generators is in-phase with the load current, while that of the other is orthogonal to it.

At 2φ=0, the currents are equal, and with increasing φ, the consumed current of the second generator (for which the sign of φ coincides with the sign of χ) begins to grow and reaches a maximum at the point 2φ=45^0, where $2\varphi=\chi \; or \; \varphi=\chi/2$, after which it begins to fall. The consumed current of the first generator, for which the sign of φ is opposite to the sign of χ, decreases monotonically over the entire interval from 2φ=0 to $2\varphi=\chi$. At 2φ=90^0 (i.e. when $\varphi=\chi$, the output current and voltage of the second generator are in phase), the consumed current of the second generator takes the same value as at 2φ=0, which corresponds to operation on a purely resistive load, and the consumed current of the first generator becomes zero, which corresponds to its operation on a purely reactive load. In this case, for the second generator $\chi-\varphi=0$, and for the first, $\chi-\varphi=90^0$, which makes the active component of the reduced load impedance and the consumed current of the first generator zero according to expression (11). With a further increase in φ, the consumed current for the second generator becomes negative and the generator operates on a load whose resistive part is negative. The consumed power for the first generator also becomes negative in this case, i.e. the generator recuperates part of the total oscillatory energy into the power source. Due to this, the efficiency of the OPA, defined as the ratio of the output power to the consumed power, will be close to unity throughout the entire SMC (from 2φ=0 to 2φ=180^0).

Then, with increasing φ, the negative consumed current of the first generator initially increases in magnitude, reaching its maximum at $2\varphi = 3\chi / 2$, $(2\varphi = 135^0)$, and then decreases and turns to zero at $2\varphi=180^0$. The consumed current of the second generator in the section from $2\varphi=90^0$ to $2\varphi=180^0$ monotonically decreases to zero. The theoretical dependencies plotted in Figure 9 have been experimentally confirmed.

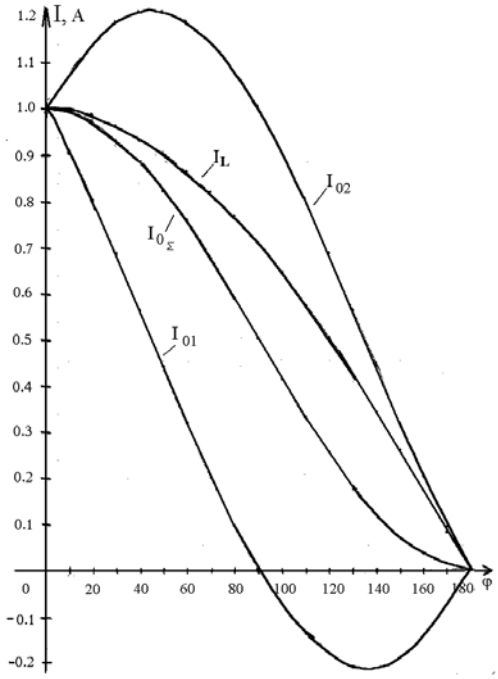


Figure 9. Theoretical dependencies of generator currents

As can be seen from Figure 9, the total current consumed by both generators has a maximum at the common-mode point (φ = 0) and decreases monotonically with increasing phase shift. It should be noted that the transistor pulse currents (in the form of half-wave cosine wave sections with different phases) have identical maximum values for all four transistors of both channels, since a common load current flows through the transistors. The load current amplitude is determined by the supply voltage E, the phase shift of the channel signals φ, and the absolute value of the load impedance, according to (7). Accordingly, all four transistors of the OPA output stage are, from a safety standpoint, in completely identical conditions: they have identical maximum currents and voltages at the drains, identical dissipated powers (and even identical ratios between the commutative and resistive components of power loss).

At the same time, when OPA designing, it is of course necessary to take into account the possible magnitude of the load mismatch (antenna-feeder path) [27]. As follows from Figure 9, the maximum transistor loading occurs during in-phase operation of the channels (φ =0), when the output, consumed, and dissipated powers in the transistors are at their maximum; at this point, the transistor pulse currents are also at their maximum. Accordingly, the calculation of the OPA output stage mode, ensuring the safe operation of the active devices, can be carried out using traditional [24] methods.

Conclusions

An analysis of the channel generators operating characteristics in outphasing high-efficiency radio-frequency power amplifiers demonstrated the advantage of using Voltage Mode Class D (VMCD) switching generators with filter loads (FL) based on field-effect (FET) transistors – MOSFET, VDMOS, LDMOS, and GaN HEMT. Based on equivalent circuits and currents and voltages diagrams, basic expressions were derived

for calculating output power, power loss, efficiency, and maximum currents when operating with matched and mismatched (complex) loads. The presence of inverse currents was demonstrated, and their maximum values, achievable with a 45-degree phase shift, were determined, which are necessary for component selection. Further work will focus on accounting for switching losses.

REFERENCES

[1] H. Chireix, “High power outphasing modulation,” *Proc. IRE*. 1935, no. 23, pp. 1370-1392.

[2] S.A. Hetzel, A. Bateman, J.P. McGeehan, “Linc transmitter,” *Electronics letters*. 9th May 1991. Vol. 27, no. 10, pp. 133-137.

[3] Q. F. Ngo and O. V. Varlamov, “Outphasing Transmitter Circuit with Switching Generators Direct Summation: Static Mode Analysis,” *2025 Wave Electronics and its Application in Information and Telecommunication Systems (WECONF)*, St. Petersburg, Russian Federation, 2025, pp. 1–9, doi: 10.1109/WECONF65186.2025.11017168.

[4] Q. F. Ngo, N. S. Bekushev, V. N. Gromorushkin, O. V. Varlamov, “Outphasing transmitter circuit with switching generators direct summation design features,” *T-Comm*, 2025, vol. 19, no. 2, pp. 4–14. DOI: 10.36724/2072-8735-2025-19-2-4–14.

[5] V. N. Gromorushkin and O. V. Varlamov, “Dynamic Operation Modes of Outphasing Transmitters with Switching Generators Direct Summation,” *2025 Wave Electronics and its Application in Information and Telecommunication Systems (WECONF)*, St. Petersburg, Russian Federation, 2025, pp. 1–7, doi: 10.1109/WECONF65186.2025.11017153.

[6] O. V. Varlamov and V. N. Gromorushkin, “Mismatched Load Operation of Outphasing Transmitters with Switching Generators Direct Summation,” *2025 Wave Electronics and its Application in Information and Telecommunication Systems (WECONF)*, St. Petersburg, Russian Federation, 2025, pp. 1–5, doi: 10.1109/WECONF65186.2025.11017139.

[7] Q.F. Ngo, V.N. Gromorushkin, O.V. Varlamov, “Outphasing transmitters with switching generators direct summation: dynamic modes and mismatched load operation,” *T-Comm*, 2025, vol. 19, no. 3, pp. 13–23. DOI: 10.36724/2072-8735-2025-19-3-13–23.

[8] O. V. Varlamov, “Experimental Study of a Synchronous DVB-T2 Network in the Yaroslavl Region. Problems with Some Manufacturers' Receivers,” *2020 International Conference on Engineering Management of Communication and Technology (EMCTECH)*, Vienna, Austria, 2020, pp. 1 - 4, Doi: 10.1109/EMCTECH49634.2020.9261562.

[9] O. Varlamov, V. Varlamov, and A. Dolgopyatova, "Digital Radio Broadcasting Network in the Arctic Region", *2019 24th Conference of Open Innovations Association (FRUCT)*, Moscow, Russia, 2019, pp. 457-462. DOI: 10.23919/FRUCT.2019.8711933.

[10] O. V. Varlamov, and A. A. Bychkova, "Basis of Technical Design and Development a Single-Frequency DRM Digital Broadcasting Network for Venezuela", *2021 Systems of Signal Synchronization, Generating and Processing in Telecommunications (SYNCHROINFO*, 2021, pp. 1-7, doi: 10.1109/SYNCHROINFO51390.2021.9488396.

[11] A.A. Losev, “Development and analysis of technical solutions for a satellite repeater power amplifier built using the outphasing method,” Ph.D. Thesis, MTUCI, Moscow, Russia, 2017.

[12] A. Pastukh, V. Tikhvinskiy, S. Dymkova, and O. Varlamov, “Challenges of Using the L-Band and S-Band for Direct-to-Cellular Satellite 5G-6G NTN Systems,” *Technologies*, vol. 11, no. 4, p. 110, Aug. 2023, Doi: 10.3390/technologies11040110.

[13] V. Tikhvinskiy, A. Pastukh, S. Dymkova, O. Varlamov, “Compatibility Analysis Between RedCap Non-Public Networks and 5G NR in TDD FR1 and FR2 Bands,” *Inventions*, 2025. 10 (1), 12. https://doi.org/10.3390/inventions10010012.

[14] O. Varlamov, D. C. Nguyen, and A. Grebennikov, “Broadband and Efficient Envelope Amplifier for Envelope Elimination and Restoration/Envelope Tracking Higher-Efficiency Power Amplifiers,” *Sensor*s, vol. 22, no. 23, p. 9173, Nov. 2022, Doi: 10.3390/s22239173.

[15] O.V. Varlamov, “Powerful broadband DC amplifiers for modulation path of transmitters with separate amplification,” *T-Comm*. 2022. vol. 16, no.11, pp. 4-14. DOI: 10.36724/2072-8735-2022-16-11-4-14

[16] Nguyen, Dang Canh, Victor N. Gromorushkin, and Oleg Varlamov. 2023. “Theoretical Comparison of Different Envelope Elimination and Restoration Transmitter PWM Modulator Configurations to Expand the Possible Antenna Mismatch,” *Sensors* 23, no. 23 : 9466. https://doi.org/10.3390/s23239466.

[17] D.C. Nguyen, O.V. Varlamov, "Simulation model for studying the operation of switching mode envelope elimination and restoration RF power amplifiers for a narrow-band load", *H&ES Research*. 2022. Vol. 14. No 2, pp. 10-18. doi: 10.36724/2409-5419-2022-14-2-10-18.

[18] O.V. Varlamov, D.C. Nguyen, S.E. Grychkin, “Combination of synthetic high-performance RF amplification techniques,” *T-Comm*. 2021. vol. 15, no.9, pp. 11-16. DOI: 10.36724/2072-8735-2021-15-9-11-16.

[19] Q.F. Ngo, O.V. Varlamov, “Engineering and technical principles of highly effective linear radio transmitters construction for HF manpack radios,” *T-Comm*, 2024, vol. 18, no. 4, pp. 4–14. DOI: 10.36724/2072-8735-2024-18-4-4-14.

[20] Q. F. Ngo and O. V. Varlamov, "Methods for Increasing the Efficiency of Amplitude-Phase Modulated Signals Power Amplifiers," *2024 Systems of Signals Generating and Processing in the Field of on Board Communications*, Moscow, Russian Federation, 2024, pp. 1-8, doi: 10.1109/IEEECONF60226.2024.10496778.

[21] O.V. Varlamov, V.N. Gromorushkin, V.B. Kozyrev, A.V. Melanin, “Addition of the power outputs from push-pull voltage-switching oscillators having a resistive load,” *Radioelectronics and Communications Systems*. 1989, vol. 32. no 7, pp. 30-35.

[22] R.Yu. Ivanyushkin, “Research and development of a high-frequency path of a radio broadcasting MF transmitter built using the outphasing method,” Ph.D. Thesis / Moscow Technical University of Communications and Informatics. Moscow, 2001.

[23] V.B. Kozyrev, V.G. Lavrushenkov, V.P. Leonov, “Transistor generators of harmonic oscillations in the switching mode,” Moscow: Radio and communication, 1985.

[24] O. V. Varlamov and V. N. Gromorushkin, "Class D Switching Power Amplifier with a Filter under Load Mismatch Conditions", *2020 Wave Electronics and its Application in Information and Telecommunication Systems (WECONF)*, Saint-Petersburg, Russia, 2020, pp. 1-6, doi: 10.1109/WECONF48837.2020.9131508.

[25] Q. F. Ngo and O. V. Varlamov, "GaN HEMT Transistors Application Features in Outphasing Transmitters," *2026 Wave Electronics and its Application in Information and Telecommunication Systems (WECONF)*, St. Petersburg, Russian Federation, 2026, pp. 1-6, doi: 10.1109/WECONF69969.2026.11553787.

[26] N. S. Bekushev, Q. F. Ngo and O. V. Varlamov, "Design Methods of Outphasing Transmitter Exciter for Lab Prototyping," *2026 Systems of Signals Generating and Processing in the Field of on Board Communications*, Moscow, Russian Federation, 2026, pp. 1-8, doi: 10.1109/IEEECONF68869.2026.11461172.

[27] O. V. Varlamov, "Power Capacity of HF Automatic Antenna Tuner Switched by PIN Diodes under Load Mismatch Conditions", *2020 Systems of Signal Synchronization, Generating and Processing in Telecommunications (SYNCHROINFO)*, Svetlogorsk, Russia, 2020, pp. 1-5, doi: 10.1109/SYNCHROINFO49631.2020.9166046.